



OPEN

Cross-entropy based AC series arc fault detection for more electric aircrafts

Sina Hosseini^{1,2} & Iman Sadeghkhani^{1,2}✉

The increasing adoption of More Electric Aircraft (MEA) has introduced new challenges in ensuring the reliability and safety of onboard electrical systems. Among these challenges, AC series arc faults pose a significant risk due to their potential to degrade system integrity and cause fire hazards. Detecting such faults is particularly challenging because of their intermittent nature and similarity to normal load switching events. This article proposes a novel AC series arc fault detection technique based on time-domain current waveform analysis. The technique quantifies the asymmetry introduced by arc faults using cross-entropy and extracts the fault-imposed component to derive a fault detection index. The energy of this component is monitored over time to distinguish persistent arc faults from transient disturbances. The effectiveness of the proposed technique is evaluated through extensive MATLAB/Simulink simulations. Various case studies, including load switching events, nonlinear loads, and system parameter variations, are analyzed to assess the technique's robustness. Additionally, a sensitivity analysis is conducted to investigate the impact of key parameters on detection performance. The results confirm that the proposed technique achieves high sensitivity and reliability in detecting series arc faults while effectively discriminating against non-fault disturbances, making it a promising solution for enhancing the safety and protection of next-generation aircraft electrical systems.

Keywords Cross entropy, Fault detection, More electric aircraft, Protection, AC series arc fault

List of symbols

CE_F	Cross-entropy during a fault
CE_N	Cross-entropy during normal operation
CE_{SI}	Fault-imposed component of cross-entropy
i_{arc}	Current of the series arc
K	Number of samples per cycle
L	Inductance of load
l	Arc length
F	Arc function
N	Number of samples per half-cycle
P_r	Given pressure of the gas in which the arc is formed
R_c	Corona, glowing or melted bridge resistance
R	Resistance of load
T_S	Sampling period
t_{SAFDI}	Time duration of satisfying $SAFDI > \xi$
t_w	Waiting time
v_{arc}	Voltage of the series arc
v_s	Feeding bus voltage
W	Length of the sliding data window for energy calculation
ξ	Disturbance detection threshold

Abbreviations

AC	Alternating current
ANN	Artificial neural network

¹Smart Microgrid Research Center, Najafabad Branch, Islamic Azad University, Najafabad 85141-43131, Iran.

²Department of Electrical Engineering, Najafabad Branch, Islamic Azad University, Najafabad 85141-43131, Iran.

✉email: sadeghkhani@pel.iaun.ac.ir

APU	Auxiliary power unit
ATRU	Auto-transformer rectifier unit
ATU	Autotransformer unit
CAGR	Compound annual growth rate
CNN	Convolutional Neural Network
DC	Direct current
FFT	Fast Fourier transform
IEA	International energy agency
MEA	More electric aircraft
NN	Neural Network
PDS	Power distribution system
RAT	Ram air turbine
SAFDI	Series arc fault detection index
SC	Subtractive correlation
SSPC	Solid-state power controllers
TDR	Time domain reflectometry
TNN	Transformer neural network

Background and challenges

The aviation industry is undergoing a significant transformation towards electrification, driven by mounting environmental concerns and rapid technological advancements. Figure 1 shows the share of carbon dioxide (CO₂) emissions by various sectors of transportation in 2023 where the aviation sector contributes approximately about 10% of all transportation-related emissions¹. International Energy Agency (IEA) report states that, in 2023, the aviation sector contributed 2.5% of global energy-related CO₂ emissions, experiencing faster growth between 2000 and 2019 than other transportation modes such as rail, road, and shipping². With the resurgence of international travel post-COVID-19, aviation emissions nearly reached 950 Mt CO₂, surpassing 90% of pre-pandemic levels. To achieve emission reductions in alignment with the Net Zero Emissions by 2050 Scenario, the demand for sustainable solutions has become critical³. The More Electric Aircraft (MEA) paradigm represents a significant evolution in modern aviation, characterized by the replacement of traditional hydraulic, pneumatic, and mechanical subsystems with advanced electrical systems^{4,5}. This transition is driven by the need for enhanced operational efficiency, improved reliability, and reduced environmental impact. By leveraging advancements in power electronics and high-efficiency electric motors, MEA designs enable lighter aircraft architectures and more efficient aircraft power distribution systems (PDSs). These innovations not only reduce fuel consumption but also lower greenhouse gas emissions, aligning with the aviation industry's sustainability goals^{6,7}. Furthermore, the modularity and adaptability of electrical systems facilitate easier maintenance and upgrades, contributing to lower lifecycle costs and greater system resilience. The MEA market, valued at USD 4.40 billion in 2025, is projected to grow to USD 8.19 billion by 2030, reflecting a compound annual growth rate (CAGR) of 13.22% during this period⁸.

The transition to MEA has led to a substantial increase in electrical power demands, introducing new challenges in fault detection within the aircraft PDS. One of the most critical issues is the occurrence of intermittent arc faults, which are transient phenomena often triggered by environmental factors such as in-flight vibrations, mechanical stress on aging cables, or degraded insulation⁹. These faults are notoriously difficult to replicate and diagnose after landing, complicating routine maintenance and increasing the risk of system failures or onboard fires if left undetected. Additionally, the use of higher voltage levels and distributed architectures in modern aircraft has heightened the risk and frequency of arc faults. Existing protection systems, such as thermal

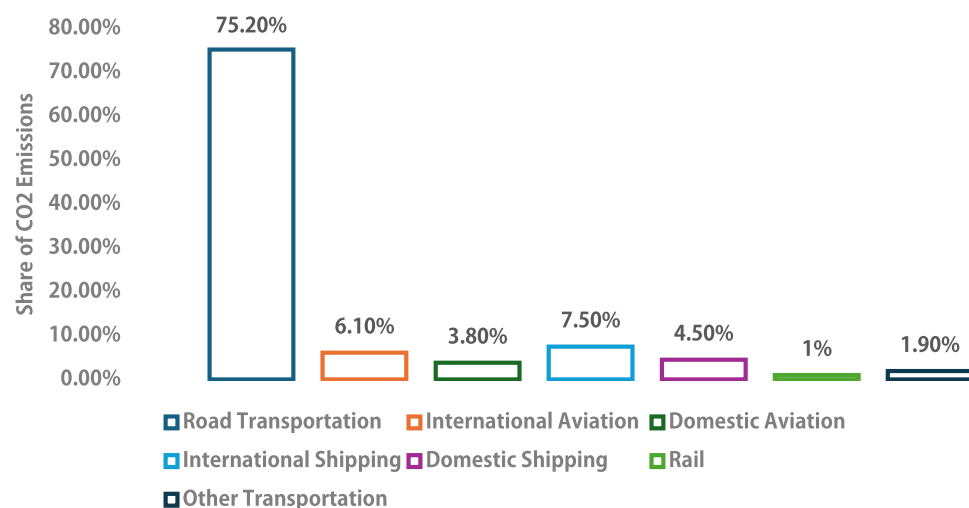


Fig. 1. Share of transport CO₂ emissions by sector in 2023¹.

circuit breakers, often fail to detect these faults due to their short duration, low magnitude, and erratic nature. To ensure safe and reliable operation, the development of an accurate and fast arc fault detection technique is imperative, necessitating advanced algorithms that can address the dynamic and complex conditions inherent in aircraft PDS.

Literature review

Based on the nature of supply voltage, arc faults can be generally classified into two categories: alternating current (AC) arc faults and direct current (DC) arc faults. Each category poses unique challenges in detection and mitigation, and several techniques have been presented to address these challenges as follows.

- *DC arc fault detection techniques* Ref. ¹⁰ introduces the transmission matrix modeling technique to develop accurate and simplified normal and faulty load circuit models and proposes an intermittent DC arc fault detection technique based on temporary deviations in load circuit coefficients and wiring parameters. A DC arc fault detection technique based on an improved LeNet5 Convolutional Neural Network (CNN) model is presented in ¹¹, which utilizes time-frequency analysis of DC currents to enhance real-time detection by leveraging the adaptive and multidimensional features of the signals. Ref. ¹² presents a generalized real-time DC arc fault detection technique that utilizes time-frequency domain features analyzed through a feed-forward Artificial Neural Network (ANN). In ¹³, a DC series arc test platform is developed for series arc optical detection in the MEA DC system, with empirical mode decomposition used to extract characteristic arc light wavelengths and wavelet transformation applied to reduce equipment noise. A machine learning technique is presented in ¹⁴ for detecting DC series arcs by analyzing a database of current signal measurements from both arc faults and nominal conditions, with a classifier implemented based on the extraction of key features from conventional current signals. Ref. ¹⁵ presents a DC series arc detection technique that monitors the fractal dimension of supply and load current and voltage waveforms for enhanced fault identification. In ¹⁶, real-time snapshot data from current and voltage transducers in radial/loop aircraft electrical systems is processed through a state estimator, which smooths the data, identifies faulty transducers, and provides optimal estimates of voltage and phase angles across the network, representing its operational state.
- *AC arc fault detection techniques* Ref. ¹⁷ presents two AC arc fault detection techniques using half-cycle data analysis, employing Fast Fourier Transform (FFT) and Wavelet Packet Decomposition (WPD) to distinguish fault currents from normal operation. A deep learning approach using a sequence-based Transformer Neural Network (TNN) model, repurposed as a sequence-to-sequence framework, is presented in ¹⁸ to detect AC arc faults by analyzing electric current windows containing at least one signal period. An enhanced technique for localizing and identifying soft faults in complex aircraft microgrid wiring networks using time domain reflectometry (TDR), the subtractive correlation (SC) method, and neural networks (NNs) is presented in ¹⁹.

Aims and contributions

The objective of this article is to develop a robust and accurate fault detection technique for AC series arc faults in MEA electrical systems to address their detection complexity due to the intermittent and low-current nature of these faults. The proposed technique analyzes the time-domain characteristics of the current waveform, using cross-entropy to quantify waveform asymmetry caused by arc faults. The energy of the fault-imposed component of the cross-entropy signal serves as the fault detection index, ensuring both sensitivity and effective discrimination against non-fault events such as load switching and nonlinear loads. To validate the effectiveness of this technique, extensive simulations are conducted in MATLAB/Simulink. The study also includes a sensitivity analysis to evaluate the impact of key parameters on detection performance. The results of this article contribute to the advancement of arc fault detection methodologies in next-generation MEA systems by improving safety and reliability in aviation electrical networks.

Article organization

The remainder of this article is organized as follows. Section 2 provides an analysis of the characteristics of AC series arc faults in MEA electrical systems, highlighting their impact on current waveforms and the challenges associated with their detection. Section 3 introduces the proposed arc fault protection technique, detailing the mathematical formulation, fault detection index, and decision-making process. The study aircraft PDS is described in Section 4. Section 5 presents the performance evaluation of the proposed technique through extensive simulations under various operating conditions, followed by a sensitivity analysis to assess the effect of key parameters on detection accuracy. Section 6 presents a discussion. Finally, Section 7 concludes the article.

Characteristics of arc faults in MEA systems

Aircraft microgrids exhibit several key differences from terrestrial microgrids ^{20,21}, primarily due to the unique operational constraints and safety requirements of aviation electrical systems:

- *Frequency characteristics* Unlike conventional terrestrial microgrids operating at 50/60 Hz, aircraft microgrids typically operate at a higher and sometimes variable frequency, often around 400 Hz, to reduce the size and weight of electrical components.
- *Compact size* Aircraft microgrids are significantly smaller in scale compared to their terrestrial counterparts due to space and weight limitations.
- *Uninterrupted power supply*: Ensuring continuous power delivery to critical loads is of utmost importance in aircraft electrical networks, far exceeding the reliability requirements of conventional terrestrial distribution systems.

- **Islanded operation** The aircraft electrical system operates in a permanently islanded mode, with no external grid connection, making self-sufficiency a critical design factor.
- **High-reliability protection** Fault protection in aircraft electrical systems demands exceptionally high reliability, as any failure must be managed without compromising the safety and operation of the aircraft.

In aircraft electrical systems, several types of faults can occur, each posing unique challenges to system stability and safety. The most common types are open circuits, short circuits, and arc faults. Arc faults, in particular, have become a growing concern due to their potential to cause significant damage and compromise aviation safety¹⁷. An arc fault occurs when electricity breaks down a typically nonconductive medium, like air, generating high-temperature plasma discharges that can melt insulation, ignite fires, and endanger aircraft cables and equipment²². Figure 2 presents a statistical analysis of the causes and locations of arc faults within the aircraft PDS. The data reveals that over one-third of these faults stem from insulation failures in the affected equipment. This highlights the critical importance of detecting arc faults in wiring systems to enhance overall safety and reliability.

Arc faults can be categorized into three main types based on their location and cause: series, parallel, and ground arc faults¹¹. Series arc faults occur due to loose or poor connections in the electrical system and are more challenging to detect because they result in small current changes that often go unnoticed by conventional circuit breakers¹⁸. Parallel arc faults, which resemble short circuits between wires or between wires and electrical structures, cause a significant increase in current, making them easier to detect by conventional protection systems. Ground arc faults, on the other hand, typically occur between the cable and the chassis of the aircraft. Each type of arc fault exhibits distinct characteristics, such as high-frequency noise, changes in the rate of current rise (di/dt), voltage drops, and sudden voltage spikes¹⁰. These unique signatures make arc fault detection a complex but critical task. Due to the subtle and erratic nature of series arc faults, they are the subject of extensive research aimed at improving detection accuracy and ensuring timely fault isolation to prevent system damage or catastrophic incidents.

AC series arc modeling

Figure 3 shows a simple single-phase equivalent AC circuit with two parallel RL loads, where a series arc fault occurs in the load lateral. The arc fault circuit can be modeled as

$$v_s = Ri_{\text{arc}} + L \frac{di_{\text{arc}}}{dt} + v_{\text{arc}}, \quad (1)$$

where v_s is the feeding bus voltage, R and L are the resistance and inductance of load, and v_{arc} and i_{arc} are the voltage and current of the series arc, respectively. Arc voltage can be related to the arc current as⁷

$$v_{\text{arc}} = F(i_{\text{arc}}) = \frac{\alpha R_c i_{\text{arc}}}{\arctan(\beta i_{\text{arc}}) i_{\text{arc}} R_c + \alpha}, \quad (2)$$

where R_c is the corona, glowing or melted bridge resistance, F is the arc function, and

$$\alpha = f(l, P_r), \quad \beta = g(l, P_r), \quad R_c = h(l, P_r), \quad (3)$$

where l is the arc length, P_r represents the given pressure of the gas in which the arc is formed. A widely used method involves defining the functions f , g , and h as bilinear expressions dependent on l and P_r . These functions

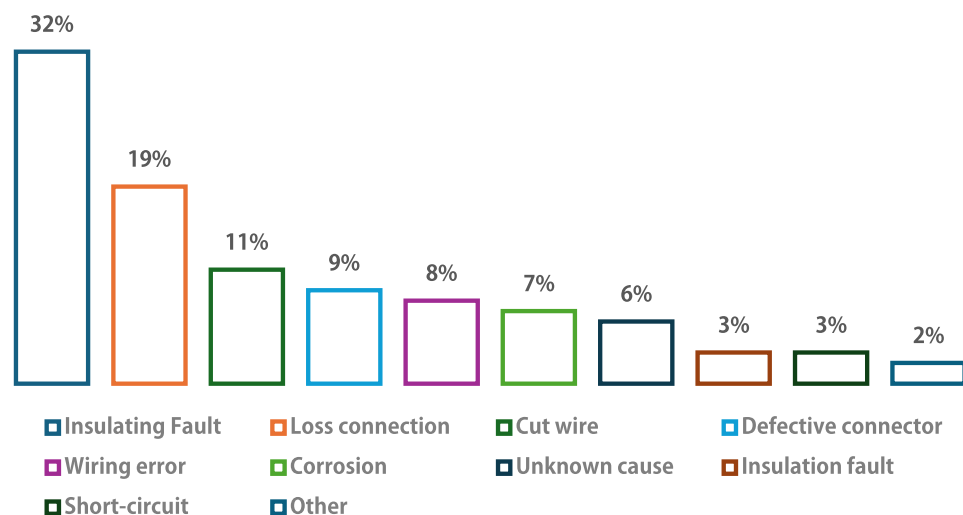


Fig. 2. Causes and locations of arc faults within the aircraft PDS⁷.

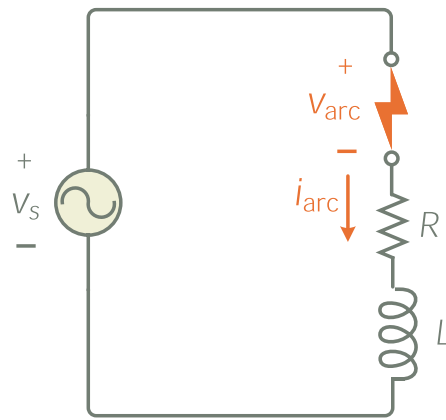


Fig. 3. Single-phase equivalent AC circuit with series arc fault.

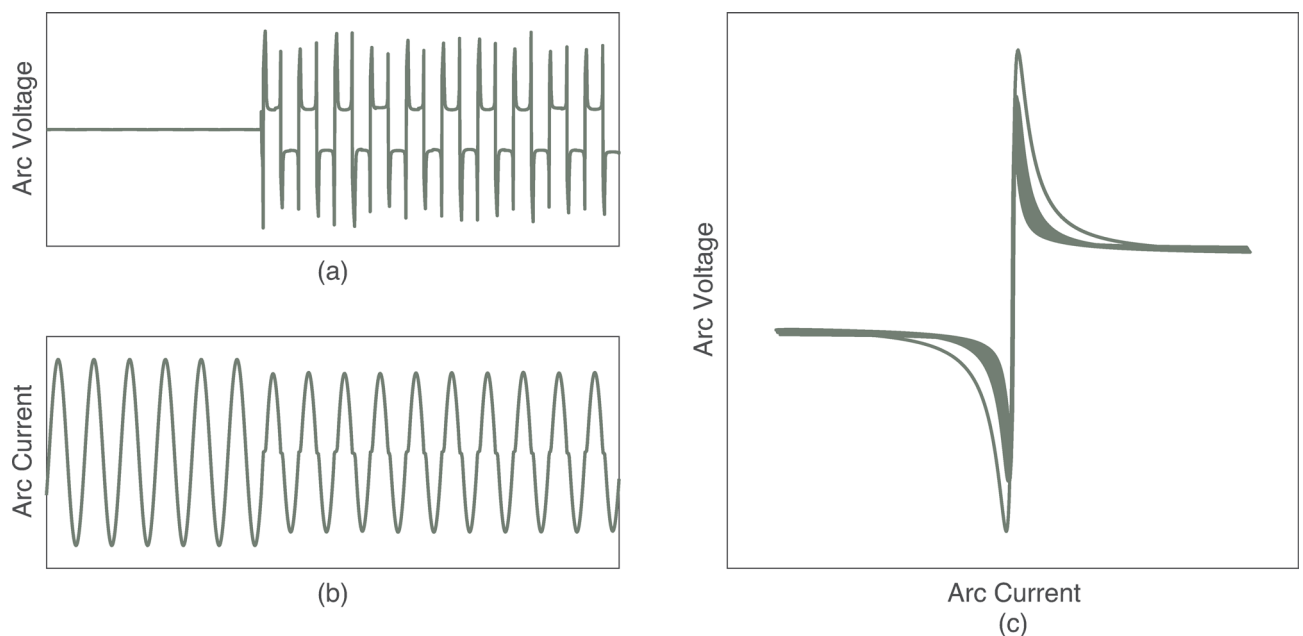


Fig. 4. Simulation of AC series arc fault model. (a) Arc voltage, (b) arc current, and (c) voltage-current characteristic of arc.

are then calibrated using either experimental data or previously published studies, where the characteristics of the system are analyzed under varying conditions, including different materials and gases. According to ⁷, in this paper, $\alpha = 49$, $\beta = 1.46$, and $R_c = 2221$ are considered that are varied around this baseline during the simulation to simulate the intermittent nature of the arc faults.

Figure 4 shows the simulation of the AC series arc fault model in the simple circuit of Fig. 3. When the arc fault occurs, the resultant arc voltage and current signals are distorted. However, load current amplitude has no significant change during the fault period, making conventional current magnitude based protective devices ineffective.

Proposed arc fault protection technique

Basic principle

Due to the random nature of arc occurrence and the compact layout of cables in the aircraft PDS, monitoring arc fault voltage is not a practical approach. Measuring voltage along all cables is highly challenging, making it an unsuitable parameter for fault detection. Instead, arc fault detection and diagnosis rely on analyzing variations in the arc fault current, which provides a more accessible and reliable indicator of fault conditions within the circuit ¹⁷. To protect the aircraft PDS against fault currents, a conventional overcurrent based protective device such as a fuse can be adopted. Fuse is self-activating, cost-effective, compact, and highly reliable, capable of interrupting fault currents without the need for sensors or actuators. However, its primary drawback is that it

can only be used once and requires manual replacement after activation²³. In modern aircraft, Solid-State Power Controllers (SSPCs) have gained significant attention due to their enhanced reliability, reduced weight, and advanced power management capabilities. These semiconductor-based switching devices are rapidly replacing traditional electromechanical circuit breakers and relays, enabling smarter, faster, and more efficient power distribution in aircraft PDS. The global SSPC market was valued at USD 476.9 million in 2023 and is projected to grow at a CAGR of 9.48% through 2029, driven by the increasing adoption of MEA and the need for more efficient and intelligent power management solutions²⁴. Figure 5 shows the block diagram of the SSPC. SSPCs utilize MOSFETs, IGBTs, or JFETs as their core switching elements, controlled via microcontrollers that enable real-time fault protection, remote control, and system diagnostics¹⁷. The SSPC microcontroller acquires output current measurements through a dedicated sensing resistor. Any inaccuracies in signal acquisition due to sensor limitations, noise, or sampling constraints can degrade the performance of detection algorithms, particularly those relying on waveform asymmetry metrics. The key advantages of SSPCs include instantaneous trip capability (25 ms), small size, high reliability, and the ability to monitor load voltage and current¹⁰. Additionally, SSPCs can be placed close to the loads, minimizing wiring length, weight, and energy losses, while enhancing overall system efficiency. Integrated within an intelligent power controller, SSPCs provide automated power distribution management, ensuring robust system performance in modern aircraft.

The low magnitude of series arc fault current as well as the short duration and intermittent nature of this fault makes fault detection in aircraft PDS a challenging task for MEA engineers. While SSPCs effectively protect against short circuits, overloads, and some arc faults, they struggle with detecting and mitigating series arc faults, which require specialized detection techniques¹¹. To address this limitation, this article proposes a new algorithm that can be implemented in the SSPCs of the aircraft PDS. The proposed technique is based on feeder current waveform processing to detect series arc faults in aircraft electrical systems. Specifically, it utilizes the cross-entropy index, a powerful metric capable of quantifying subtle variations in the waveform. This index enhances fault detection by effectively capturing low-amplitude, random, and transient signal changes, which are characteristic of series arc faults in aircraft. Unlike conventional techniques, cross-entropy provides a more sensitive and quantitative approach, making it particularly well-suited for detecting faults with low current magnitudes that are often undetectable by conventional protective devices.

Cross-entropy based arc fault detection

The nonlinearity and intermittent nature of series arc faults, lead to waveform distortions in the current signal. These distortions cause sequential half-cycles of the current waveform to differ. Cross-entropy index, a well-known statistical measure in information theory, quantifies the difference between two probability distributions. This index measures how much the waveform distribution under faulty conditions deviates from the normal operation state. The key advantage of the cross-entropy index is its ability to detect small and irregular waveform perturbations, making it highly suitable for detecting low-current arc faults in aircraft electrical networks. Among several candidate features considered—such as skewness, kurtosis, Kullback-Leibler divergence, and Teager-Kaiser energy—the cross-entropy method was found to be the most effective due to its high sensitivity to non-periodic distortions and strong robustness against non-fault disturbances like load switching and non-linear loads. In this article, the cross-entropy index is utilized as a time-domain approach to numerically characterize the subtle distortions in the current waveform caused by arc faults in aircraft PDSs. The deviation in cross-entropy values over time serves as a fault indicator.

To extract meaningful features for fault detection, the current waveform is sampled at 60 kHz, ensuring sufficient resolution to capture waveform variations. Each cycle of the 400 Hz aircraft PDS is considered as a data window, as shown in Fig. 6, containing 150 samples per cycle. The current vector is defined as:

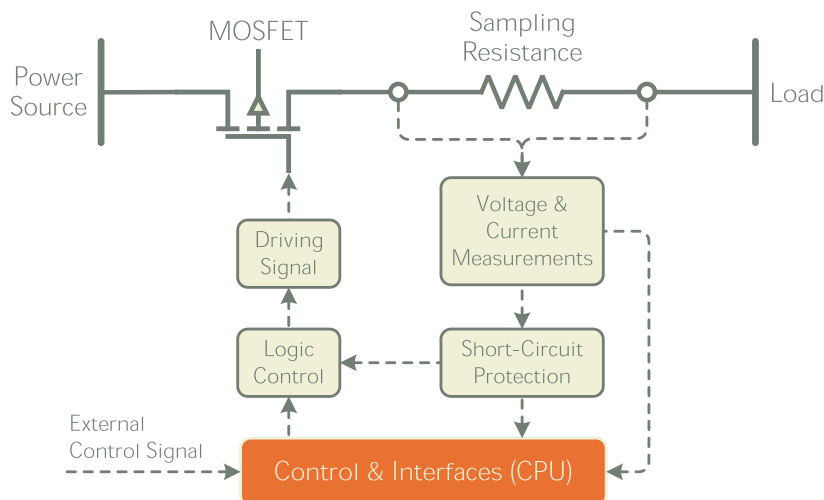


Fig. 5. Block diagram of SSPC¹¹.

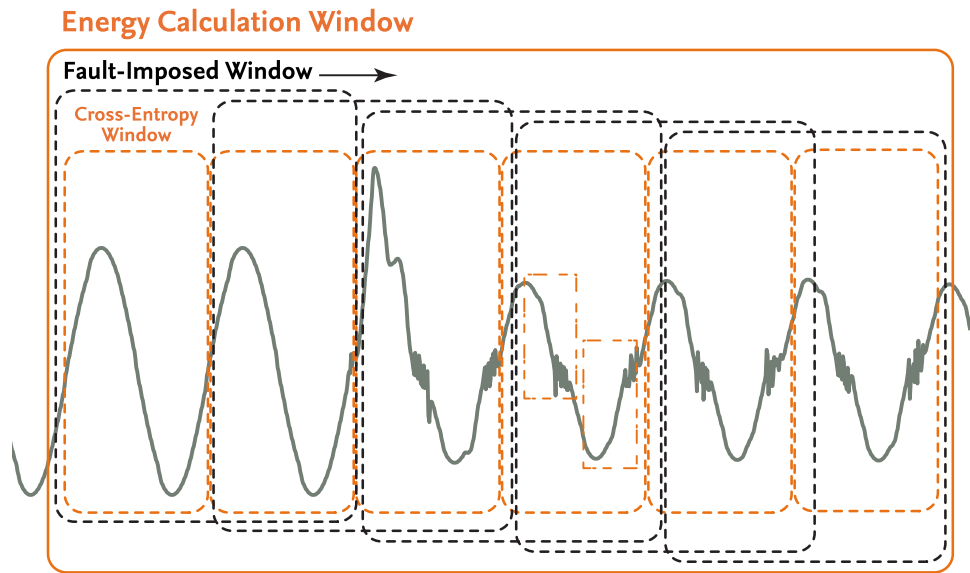


Fig. 6. Calculation windows of the proposed technique.

$$I = [i(t_0 + T_S), i(t_0 + 2T_S), \dots, i(t_0 + KT_S)], \quad (4)$$

where T_S is the sampling period, and K represents the number of samples per cycle. To analyze the nonlinearity introduced by arc faults, each cycle is split into two half-cycles, forming two current vectors:

$$\begin{aligned} I_1 &= [i(t_0 + T_S), \dots, i(t_0 + (K/2)T_S)], \\ I_2 &= [i(t_0 + (K/2 + 1)T_S), \dots, i(t_0 + KT_S)]. \end{aligned} \quad (5)$$

After forming these vectors, normalization using the L2-norm is applied as

$$\begin{aligned} \tilde{I}_1 &= \frac{I_1}{\|I_1\|_2}, \\ \tilde{I}_2 &= \frac{I_2}{\|I_2\|_2}, \end{aligned} \quad (6)$$

where $\|I_{1/2}\|_2$ represents the L2-norm of the current vector for a half-cycle.

The difference between the two sequential half-cycle vectors is quantified using the cross-entropy function, given by²⁵

$$CE(\tilde{I}_1, \tilde{I}_2) = - \sum_{r=1}^N \tilde{I}_1(r) \log \tilde{I}_2(r), \quad (7)$$

where $N = K/2$ represents the number of samples per half-cycle. A sliding window approach is used, shifting by one cycle, ensuring real-time monitoring of arc fault characteristics. Under normal operating conditions, the current waveforms in consecutive half-cycles remain similar, leading to consistent CE values. However, during a series arc fault, nonlinearities cause the half-cycle waveforms to differ, resulting in a significant increase in cross-entropy values.

As mentioned, the cross-entropy value increases from a non-zero value to another non-zero value, making the fault detection threshold a challenging task in various aircraft PDSs. To enhance fault detection robustness and minimize network-dependent variations, the fault-imposed component of cross-entropy CE_{FI} is calculated as²⁶

$$CE_{FI}(kT_s) = CE_F(KT_s) - CE_N(KT_s), \quad (8)$$

where CE_F represents the cross-entropy during a fault and CE_N represents the cross-entropy during normal operation. A practical way to compute the fault-imposed component is using a delta filter, which subtracts the delayed cross-entropy signal from its current value as²⁷

$$CE_{FI}(kT_s) = |CE(KT_s) - CE((K-1)T_s)|. \quad (9)$$

This approach ensures that under normal conditions, $CE_{FI} \approx 0$, whereas during a fault, it takes nonzero values.

In the final step of the proposed technique, the energy of the fault-imposed signal is calculated as the proposed series arc fault detection index (SAFDI) as

$$\text{SAFDI} = \sum_{i=1}^W |CE_{FI}(i)|^2, \quad (10)$$

where W is the length of the sliding data window for energy calculation (in samples).

In the presence of non-fault disturbances, such as load switching, the proposed index increases momentarily during the transition to a new operating state. However, this increase is transient, and the index rapidly returns to its initial value once the system stabilizes. In contrast, when a series arc fault occurs, the inherently intermittent nature of the arc causes continuous distortions in the current waveform across successive half-cycles. These persistent waveform variations prevent the proposed index from returning to zero, keeping it nonzero throughout the entire fault duration. Unlike transient disturbances, which exhibit short-lived index spikes, an arc fault introduces sustained fluctuations, leading to a prolonged increase in the index. Thus, the key distinguishing factor between non-fault disturbances and arc faults is the temporal behavior of the index: in transient events, the index returns to zero quickly, whereas in the presence of a series arc fault, it remains elevated due to the ongoing waveform perturbations induced by the fault. Thus, a series fault condition is verified if $\text{SAFDI} > \xi$ and $t_{\text{SAFDI}} > t_w$, where ξ is the disturbance detection threshold, t_{SAFDI} is the time duration of satisfying $\text{SAFDI} > \xi$, and t_w is the waiting time.

Threshold selection

The proposed technique has three adjustable parameters. Determining appropriate values for disturbance detection threshold ξ , waiting time t_w , and window length for calculating energy W require extensive simulation studies under various operating conditions. These simulations encompass both normal system disturbances such as load fluctuations, switching transients, and harmonic distortions, and AC series arc faults. The maximum value of the ξ under normal operating conditions (i.e., in the absence of faults) and the maximum duration for which the proposed SAFDI remains above the threshold during load switching events are identified across all simulated cases. To achieve a high level of security in fault detection while minimizing false positives, ξ and t_w are set larger than these maximum values. There is a trade-off between accuracy and detection speed when selecting the window length. A longer window enhances accuracy but increases the fault detection time. Therefore, the window length is chosen to ensure a balance between precision and rapid detection, achieving both reliable fault identification and timely response. The disturbance detection threshold ξ , waiting time t_w , and window length for calculating energy W are chosen to be 0.05, 20 ms, and 5 samples, respectively. This empirical approach ensures that the algorithm maintains a high detection accuracy, remains resilient to operational uncertainties, and avoids misclassification of transient disturbances as arc faults.

Flowchart of the proposed technique

Figure 7 shows the flowchart of the proposed fault detection algorithm. The process begins with sampling the measured feeder current waveform, forming a current vector that represents one full cycle of data. Next, the sampled data are used to construct two consecutive half-cycle current vectors. After normalizing these vectors, the cross-entropy index is applied to quantify the similarity between these two half-cycles. In the next step, the fault-imposed component of the cross-entropy signal is extracted. The energy of the fault-imposed signal is calculated as the disturbance detection index. If SAFDI exceeds a predefined threshold ξ , the algorithm's timer is activated to measure the duration for which the index remains above the threshold. If this duration surpasses a set time threshold t_w , an AC series arc fault is confirmed, triggering either a trip signal or an alarm notification.

Study aircraft power distribution system

Figure 8 shows the PDS of the Boeing B787 and Airbus A380 with few modifications, which features a more advanced architecture compared to previous generations^{28,29}. The main generator in these aircraft can provide up to 1 MVA, while the auxiliary power unit (APU) generator can deliver up to 450 kVA. A key distinction in these systems is the use of a 400 VAC primary bus operating at a variable frequency range of 380–800 Hz, replacing the older 200 VAC configurations. In this paper, frequency is considered fixed at 400 Hz. The high-voltage AC bus serves as the main power source, supplying different subsystems, including a 270 V HVDC bus, a 200 V secondary AC bus, and a 28 VDC bus. Power conversion units facilitate the distribution process, with the Auto-Transformer Rectifier Unit (ATRU) converting the 400 VAC into 270 VDC, the Autotransformer Unit (ATU) stepping down the voltage for the secondary AC bus, and the Transformer Rectifier Unit (TRU) generating the 28 VDC supply. The primary PDS integrates multiple power sources, allowing power input from the main aircraft generator, APU generator, ground power, and, in emergency situations, from a Ram Air Turbine (RAT) generator. The secondary AC bus operates at 200 V. Additionally, it can supply critical DC loads through AC/DC converters if the DC bus fails. The 270 V HVDC bus is a key component in MEA designs and is commonly found in the latest configurations of the B787 and A380. The ATRU converts power from the primary AC bus to 270 VDC, primarily supplying high-power loads such as actuation motors and hydraulic pumps. The 28 VDC bus is a standard feature across all aircraft and is derived from the primary AC bus using a TRU. It supplies low-voltage DC loads, charges onboard batteries, and, in emergency conditions, can power critical AC loads through DC/AC conversion. Essential AC and DC loads may also be powered by alternative sources, such as the RAT, fuel cell stacks, or DC/DC converters operating from the 28 VDC bus.

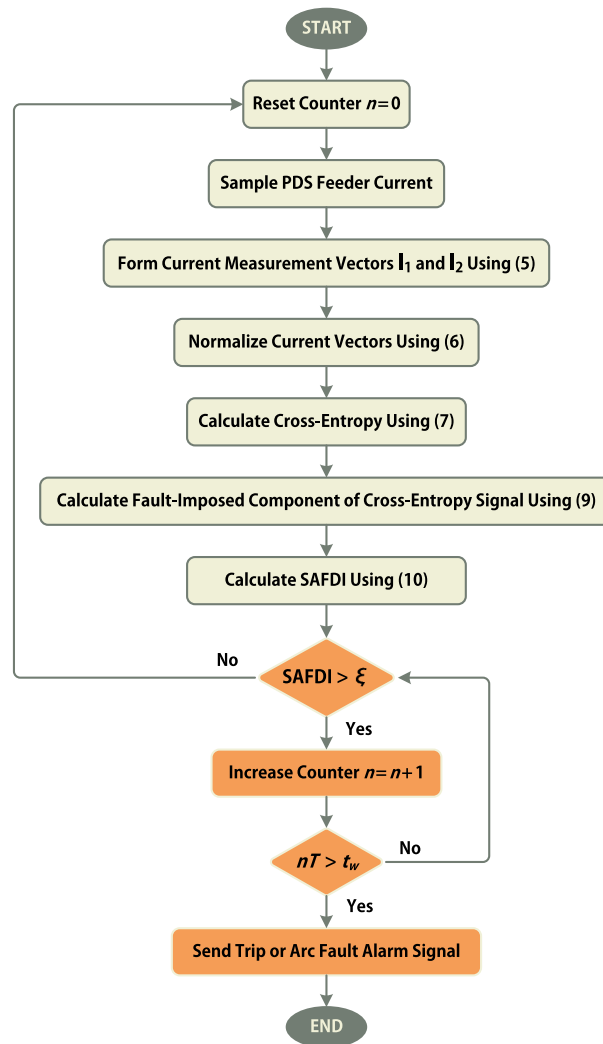


Fig. 7. Flowchart of the proposed series arc fault detection technique.

Performance evaluation

To assess the performance of the proposed fault detection technique, multiple case studies in the study test system of Fig. 8 are simulated under various operating conditions. The evaluation process considers both normal operating scenarios and arc fault conditions to ensure the security and dependability of the proposed index. The simulations are conducted using a detailed aircraft electrical system model in MATLAB/Simulink, incorporating different disturbances such as load switching and AC series arc faults. Table 1 presents the parameters of the study aircraft PDS.

Dependability assessment

In the first scenario, an AC series arc fault is introduced at the midpoint of Cable 2 in Fig. 8. The fault is initiated on phase *a* at $t = 0$ s. Figure 9 shows the simulation results for SSPC2 current signal. Since the arc fault does not cause a significant increase in current magnitude, conventional overcurrent protection devices remain inactive. However, the presence of the arc fault introduces waveform distortion in phase *a*. To quantify this distortion, the proposed fault detection index is employed. Before fault inception, the SAFDI remains close to zero. Once the arc fault occurs, SAFDI rises beyond the predefined threshold ξ , as shown in Fig. 9. At this point, the algorithm's timer is triggered to monitor the duration for which SAFDI remains above ξ . The fault condition is successfully detected at $t = 20.15$ ms. Notably, SAFDI exceeds the threshold only in phase *a*, confirming that the proposed technique accurately identifies both the occurrence of the fault and the specific faulty phase.

In the second scenario, a series arc fault is introduced at phase *b* of Cable 3, and the simulation results are presented in Fig. 10. The proposed SAFDI remains below the threshold before the fault occurs. However, upon fault inception, it exceeds the threshold exclusively in phase *b* and remains above for $t_w = 20$ ms, thereby confirming the presence of a series arc fault.

In the previous scenarios, the analysis focused on steady arc fault conditions. In the third scenario, the effectiveness of the proposed technique in detecting intermittent arc faults is examined. A series arc fault is repeatedly initiated in phase *c* of Cable 3 at $t = 0, 15$, and 22.5 ms, with each fault extinguishing after one cycle.

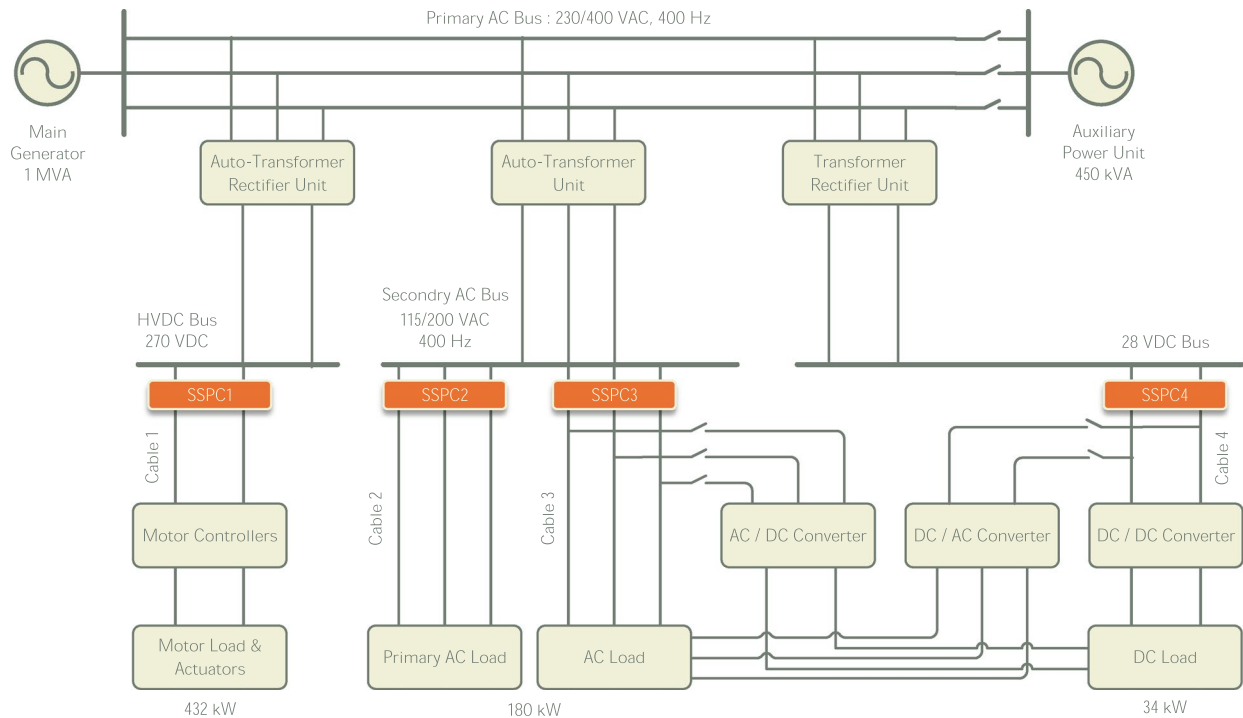


Fig. 8. Block diagram of the study aircraft power distribution system.

Parameter	Value
Nominal frequency	400 Hz
Sampling frequency	60 kHz
ATRU nominal voltage	400/270/270 V
Output filter of ATRU	$R = 0.144 \, \Omega, L = 1 \, \mu\text{H}, C = 5 \, \text{mF}$
TRU nominal voltage	400/28/28 V
Output filter of TRU	$R = 0.4 \, \Omega, L = 0.1 \, \mu\text{H}, C = 10 \, \text{mF}$
DC/DC converter control coefficients	$k_p = 1 \times 10^{-6}$ and $k_i = 1 \times 10^{-4}$
DC/DC converter filter	$L = 5 \, \mu\text{H}$ and $C = 5 \, \text{mF}$
DC/AC converter voltage control coefficients	$k_{pv} = 0.5$ and $k_{iv} = 15$
DC/AC converter current control coefficients	$k_{pi} = 5$ and $k_{ii} = 150$
DC/AC converter filter	$L = 1 \, \text{mH}$ and $C = 100 \, \mu\text{F}$
AC/DC converter control coefficients	$k_p = 1 \times 10^{-4}$ and $k_i = 5 \times 10^{-6}$
AC/DC converter filter	$L = 1 \, \mu\text{H}$ and $C = 5 \, \text{mF}$
Cable resistance and inductance	$0.11 \, \Omega$ and $5.5 \, \mu\text{H}$

Table 1. Parameters of the study aircraft PDS.

The simulation results, presented in Fig. 11, show that the proposed SAFDI remains above the threshold for more than 20 ms, successfully identifying the intermittent fault condition. It should be noted that if the time gap between two consecutive arc ignitions is sufficiently long, the SAFDI drops below the threshold, causing the proposed technique to fail in detecting the fault.

Robustness to parameter uncertainty

A critical challenge in aircraft PDS protection is the variation of system parameters over time, which can affect the accuracy of fault detection. To assess the performance of the proposed technique under such conditions, the resistance and inductance of the cables are increased by 20% to simulate aging effects and parameter fluctuations. A series arc fault is then introduced at phase *c* at the end of Cable 2. The simulation results, presented in Fig. 12, show the response of the proposed detection algorithm. The SAFDI increases significantly, surpassing the threshold ξ . It remains above this threshold for a duration exceeding t_w exclusively in phase *c*, ensuring accurate

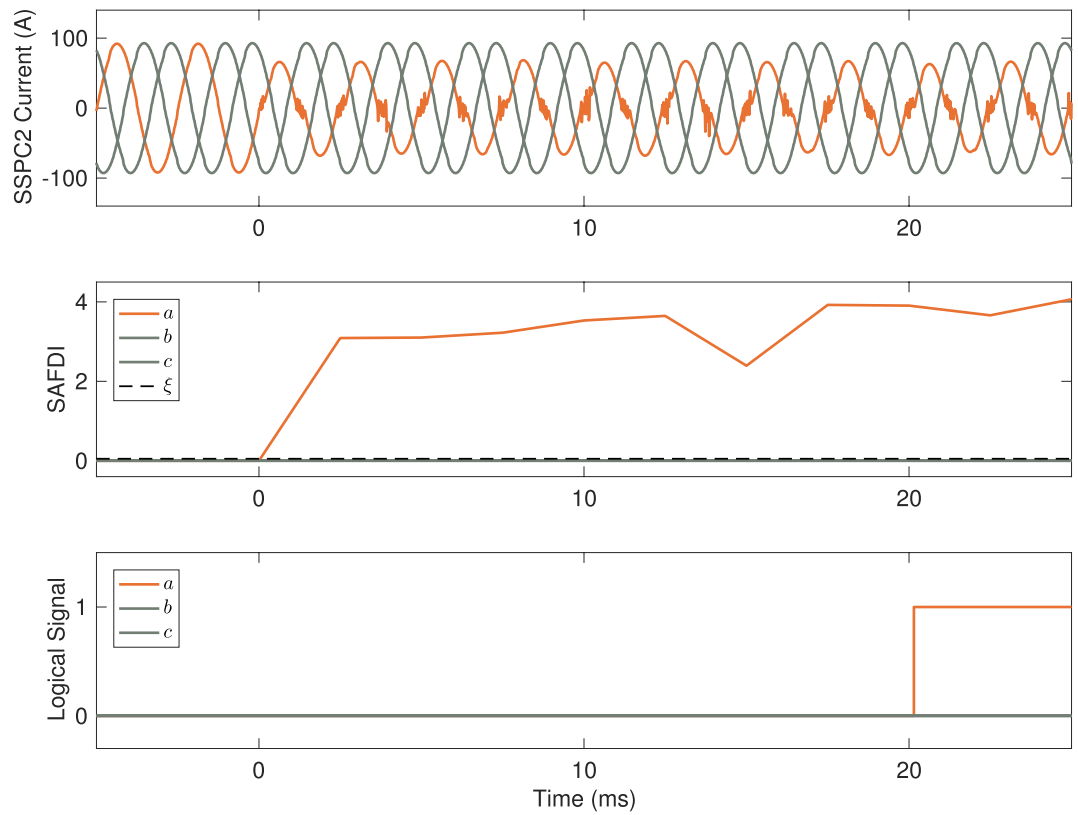


Fig. 9. Proposed SAFDI for an AC series arc fault in Cable 2.

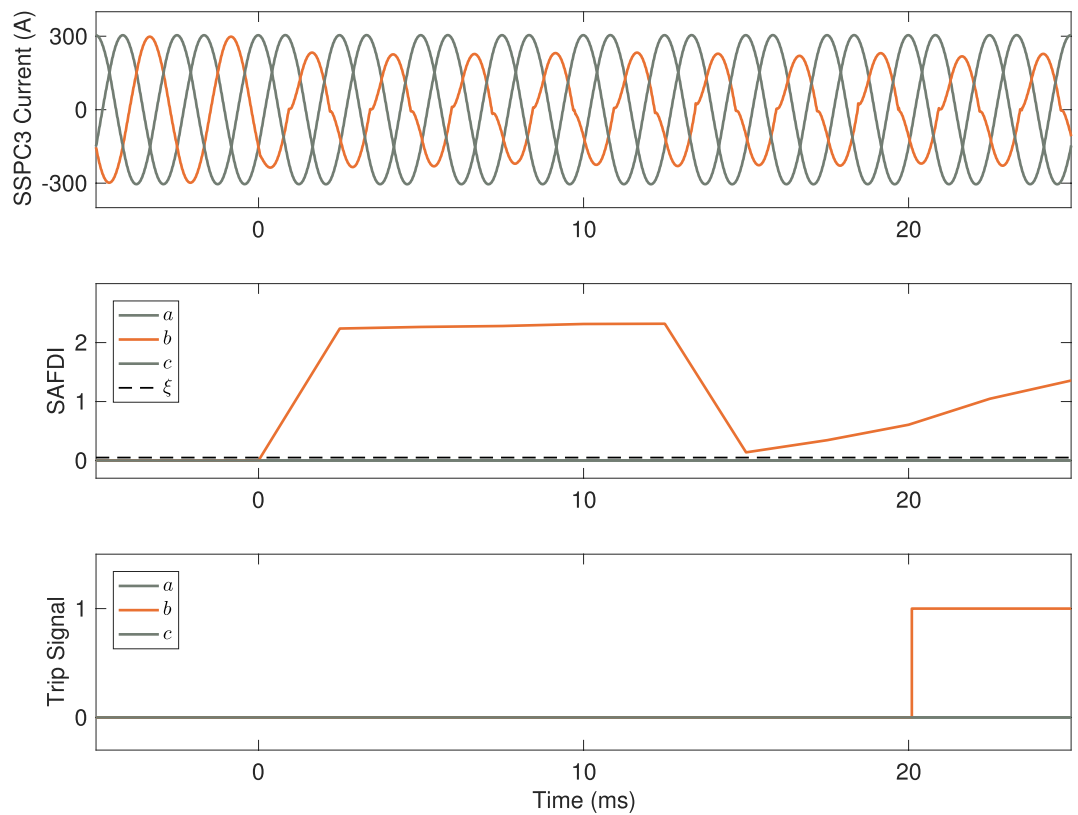


Fig. 10. Proposed SAFDI for an AC series arc fault in Cable 3.

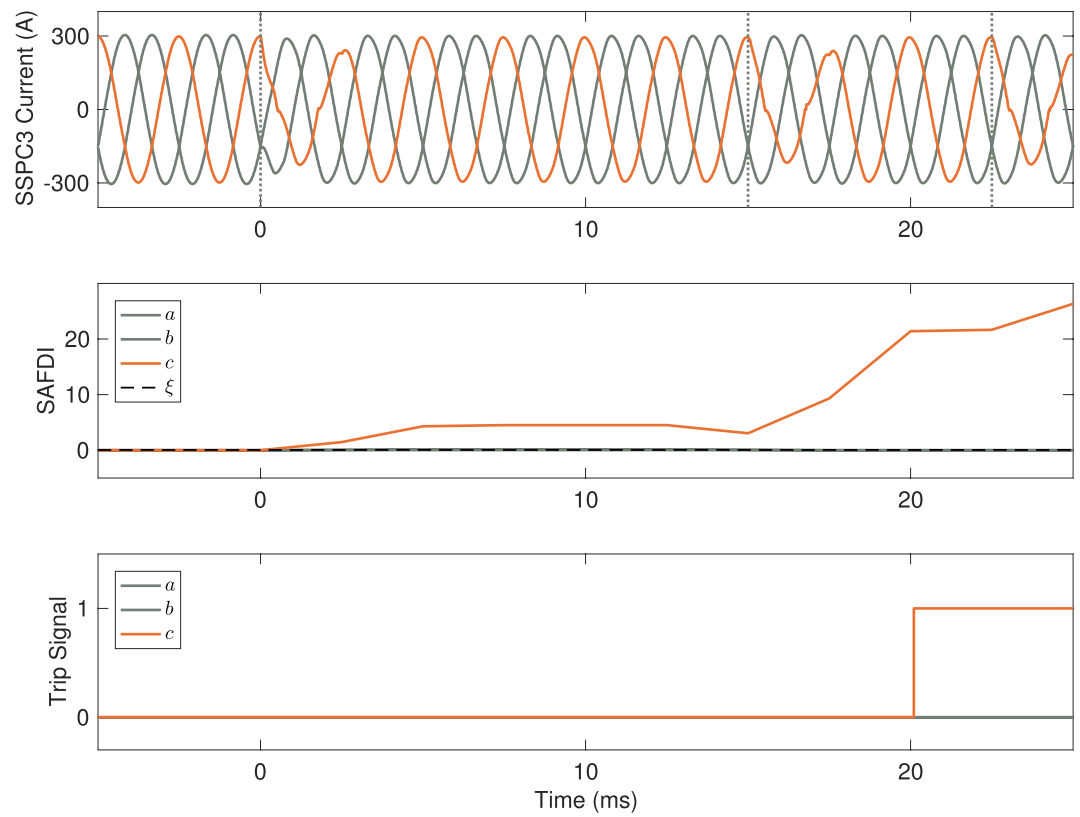


Fig. 11. Proposed SAFDI for an intermittent AC series arc fault in Cable 3.

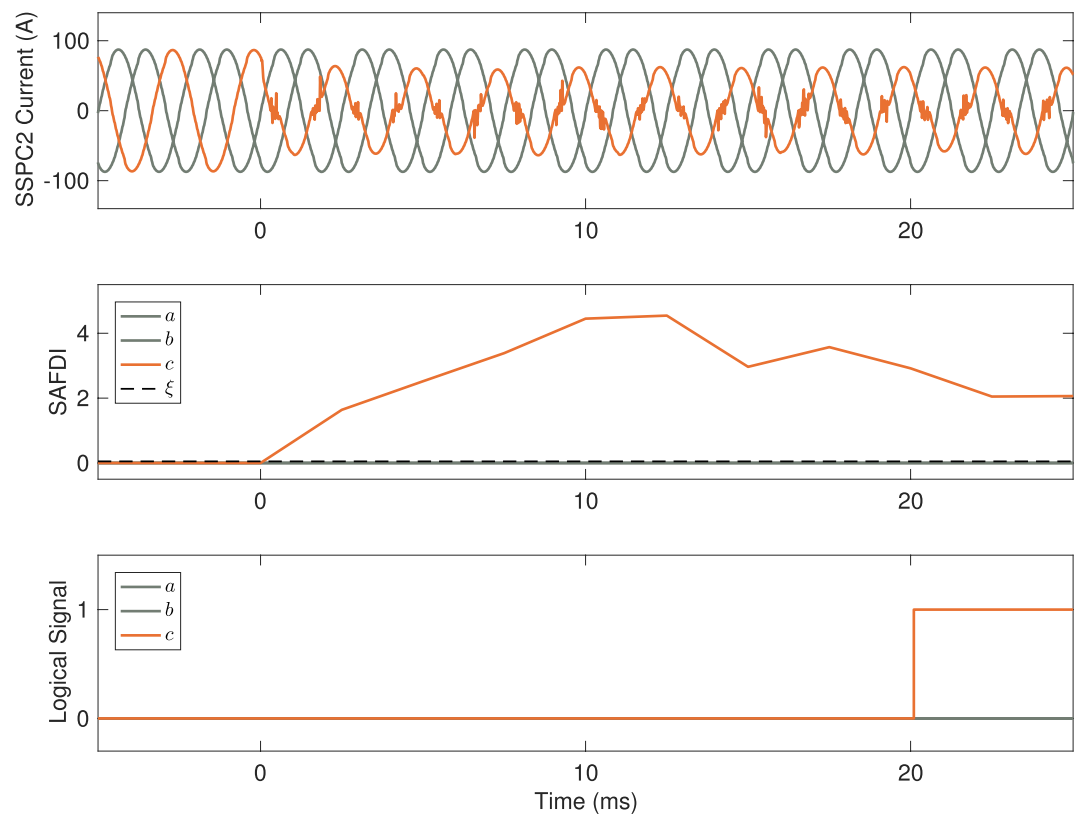


Fig. 12. Proposed SAFDI in the case of change of cable parameters.

fault detection. This scenario validates the robustness of the proposed technique in detecting series arc faults despite variations in system parameters, demonstrating its adaptability to long-term operational changes.

Security assessment

A reliable fault detection technique must remain inactive during non-fault conditions such as load switching. To assess this capability, in the first scenario, the load of Cable 3 (140 kW with a power factor of 0.8) is switched off. The simulation results, presented in Fig. 13, indicate that while the proposed SAFDI exhibits a noticeable increase, it quickly returns below the threshold across all phases before the waiting time elapses. This confirms that the proposed technique does not mal-operate under normal switching events, demonstrating its ability to distinguish between fault-induced disturbances and routine system variations.

In the next scenario, the performance of the proposed technique is evaluated in the presence of a non-linear load, which introduces waveform distortion in the current signal. To simulate this condition, a non-linear load is switched on in parallel with the load of Cable 2, where a rectifier supplies a parallel $R - C$ load. The simulation results, shown in Fig. 14, reveal that although the SAFDI temporarily exceeds the threshold in all phases, indicating a disturbance, it quickly returns below ξ before the waiting time t_w elapses. This confirms that the proposed technique effectively differentiates between fault-induced disturbances and waveform distortions caused by non-linear loads, ensuring reliable fault detection.

Sensitivity analysis

In the first scenario, a sensitivity analysis is conducted to examine the impact of the sliding data window length used for energy calculation. A series arc fault is simulated in phase b of Cable 2, and the proposed fault detection index is evaluated for different window lengths. Figure 15 presents the simulation results for $W = 2, 5, 10$, and 20. While a window length of 2 allows fault detection, the SAFDI amplitude remains close to the detection threshold, potentially affecting reliability. Conversely, a window length of 5 provides a more distinct and acceptable SAFDI amplitude, enhancing detection confidence. Increasing the window length beyond this value does not yield significant improvements in SAFDI amplitude but comes at the cost of increased computational burden and detection time.

In the second scenario, a sensitivity analysis is conducted to evaluate the impact of sampling frequency on fault detection performance. A high sampling rate is required to capture fast transient signatures of arc faults in the 400 Hz aircraft system, enabling accurate waveform analysis. A series arc fault is simulated in phase a of Cable 3, and the proposed fault detection index is computed for different sampling frequencies, including 10, 60, 100, and 200 kHz. The simulation results, shown in Fig. 16, indicate that while a sampling frequency of 10 kHz allows fault detection, the SAFDI amplitude remains close to the detection threshold, which may compromise reliability. A sampling frequency of 60 kHz provides a sufficiently high SAFDI amplitude, ensuring reliable fault

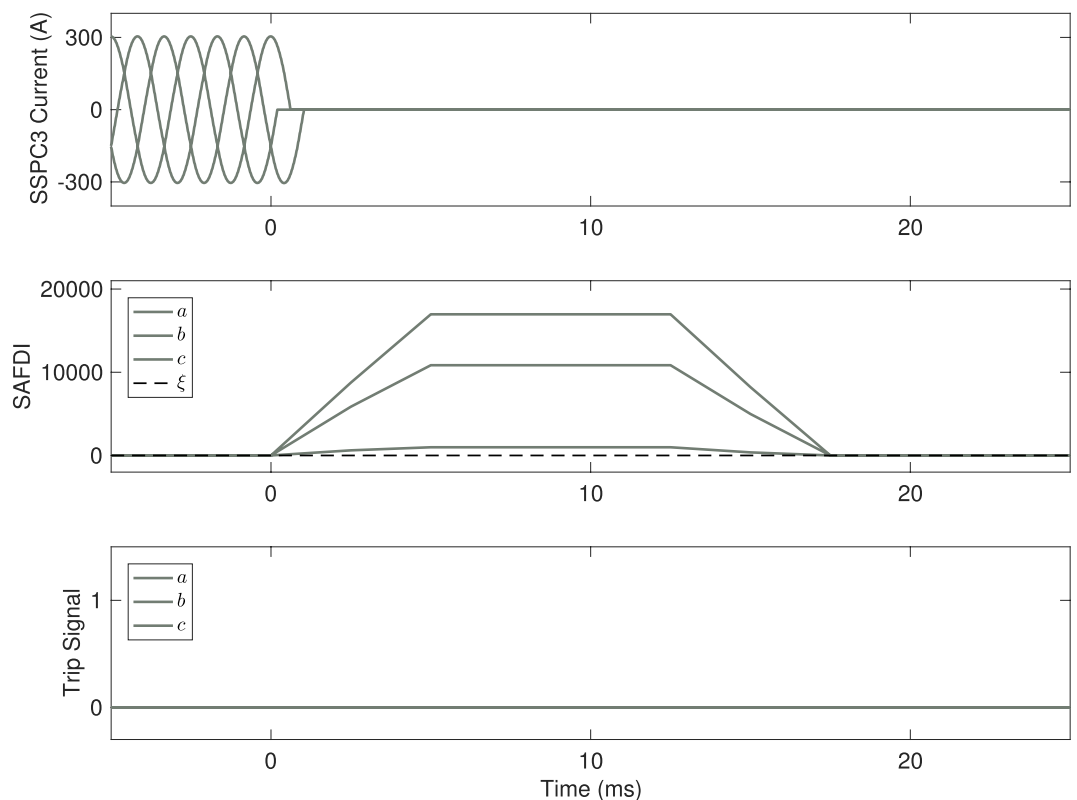


Fig. 13. Proposed SAFDI in the case of normal load switching.

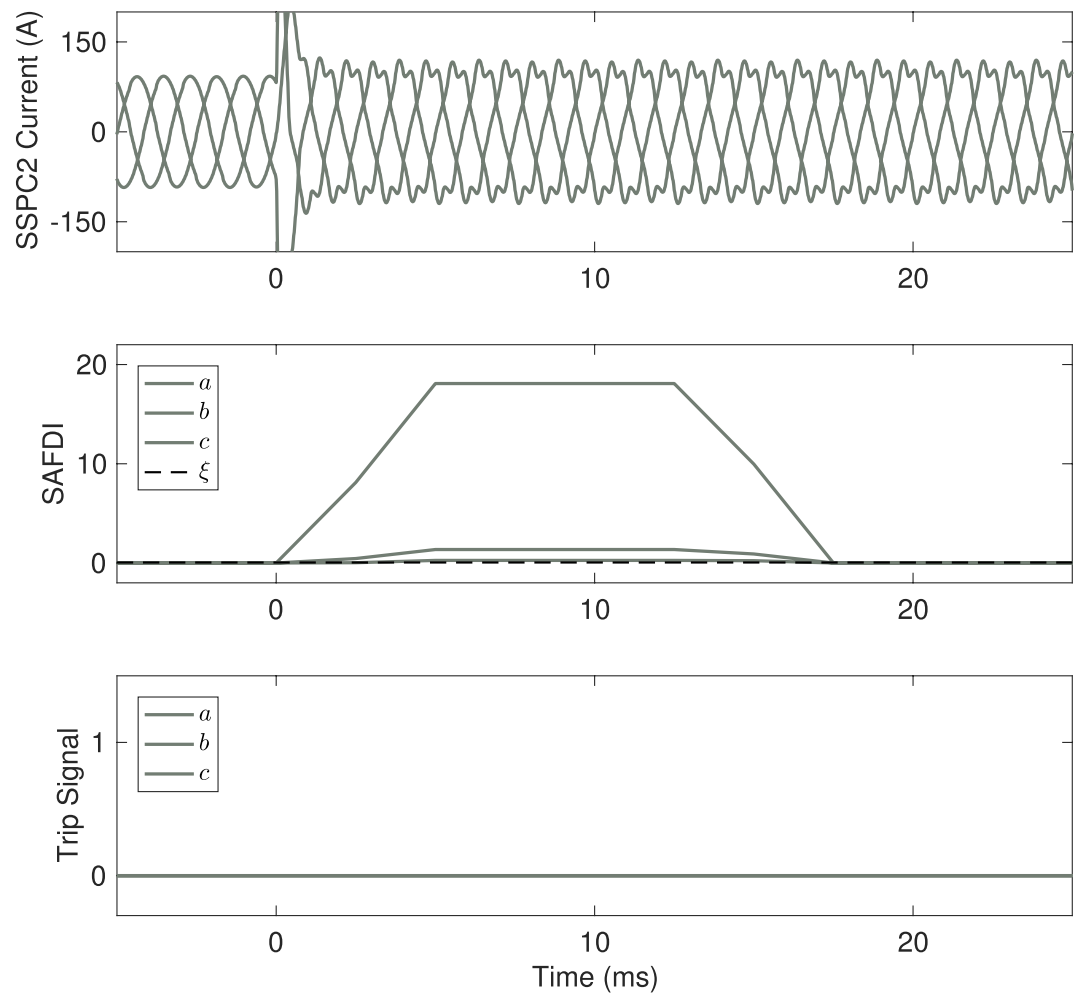


Fig. 14. Proposed SAFDI in the case of harmonic load switching.

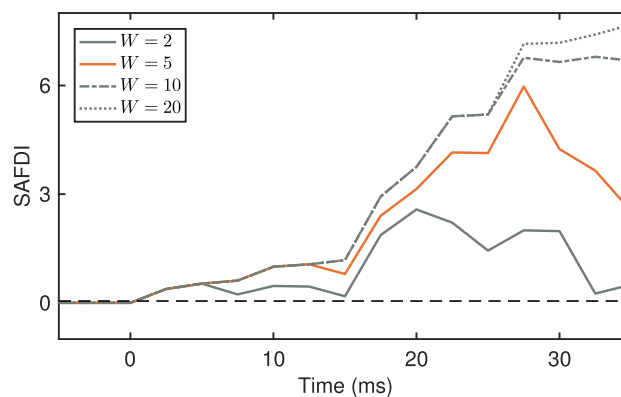


Fig. 15. Proposed SAFDI with various data window lengths.

identification. Higher sampling frequencies further enhance the robustness of SAFDI; however, they come at the cost of increased computational complexity and hardware requirements.

Discussion

Comparative assessment

The comparative assessment of the proposed SAFDI with existing AC series arc fault detection techniques is presented in Table 2. The proposed technique operates with a moderate sampling frequency and does not

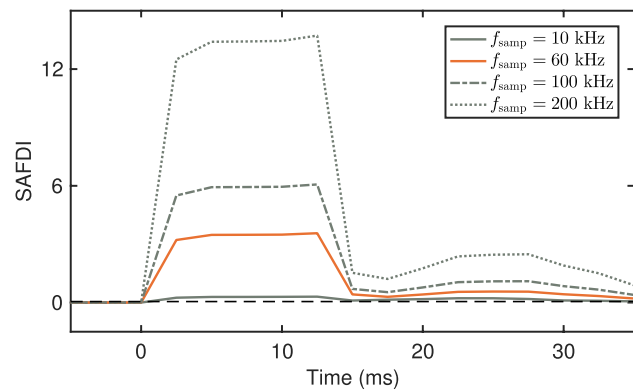


Fig. 16. Proposed SAFDI with various sampling frequencies.

	17	18	19	Proposed Technique
Technique	FFT and WPD	Deep learning using TNN	TDR, SC, and NN	Cross-entropy
Accuracy	Medium	High	High	Medium
Sampling frequency	25 kHz	100 kHz	NA*	60 kHz
Aircraft PDS frequency	400 Hz	400, 600, 800 Hz	NA	400 Hz
Arc fault detection device	SSPC	NA	NA	SSPC
Tested under non-linear load?	X	X	X	✓
No requirement for a training dataset?	✓	X	X	✓
Tested under load switching?	X	X	X	✓
Tested under parameter uncertainty?	X	X	X	✓
Determined fault location?	X	X	✓	X

Table 2. Comparison of the proposed SAFDI with some existing AC series arc fault detection techniques.

*NA: Not applicable

require a training dataset. It has been extensively tested in a 400 Hz aircraft PDS, considering critical operational conditions including non-linear loads, load switching events, and parameter variations. In contrast, many previous studies lack such comprehensive evaluations under such conditions. On the other hand,¹⁸ examines three different aircraft power system frequencies of 400, 600, and 800 Hz, and¹⁹ extends its approach to fault location determination in addition to fault identification. Moreover, artificial intelligence based techniques (^{18,19}) offer higher accuracy in fault detection compared to signal processing based techniques.

Practical considerations and experimental challenges

Conducting real-world experiments to validate the proposed arc fault detection technique in aircraft power distribution systems presents several practical challenges. One major issue is the inherent danger of electrical arcs, which can generate intense heat, sparks, and electromagnetic interference-necessitating specialized equipment and fast disconnection mechanisms to ensure safety. Moreover, replicating the actual conditions of aircraft electrical systems, which operate at 400 Hz and involve nonlinear and switching loads, requires advanced infrastructure that is often unavailable in academic environments. Additionally, producing arc faults in a stable and repeatable manner is difficult, as arc behavior is highly dependent on variables such as gap distance, electrode material, voltage, and current, and is inherently stochastic. Arc faults also generate significant electrical noise, which can affect measurement accuracy and demands the integration of robust filtering and noise mitigation techniques into the detection system.

Future work

Future studies should focus on enhancing SSPC capabilities for arc fault detection in variable-frequency aircraft PDSs, which are integral to next-generation aircraft. Additionally, improving algorithm robustness under diverse operating conditions remains essential, particularly in mitigating the effects of measurement noise and distinguishing arc faults from non-linear loads that generate second harmonic components and waveform asymmetry. Furthermore, extending the method to accurately localize the faulty segment after detection would significantly enhance fault management and system recovery. Moreover, the proposed algorithm can be extended and adapted for the detection of open and shunt fault types, including high-impedance faults, to broaden its applicability in aircraft electrical systems. Finally, future work can focus on optimizing the detection algorithm by incorporating the effects of cable material, length, and environmental conditions to enhance accuracy and reduce diagnosis time.

Conclusion

This paper presented a protection technique for detecting AC series arc faults in aircraft PDSs. The core of the proposed technique lies in cross-entropy analysis, which effectively captures waveform asymmetry caused by arc faults. To improve robustness, the fault-imposed component of the entropy signal was isolated, and its energy was formulated into a new index called the SAFDI. Extensive simulation studies were carried out to evaluate the technique under diverse scenarios. The technique was validated against various series arc fault conditions and shown to consistently detect faults with a response time of approximately 20 ms. Importantly, it demonstrated high resilience by remaining inactive during normal operational events, such as load switching and the presence of nonlinear loads, avoiding false positives. A sensitivity analysis on the sliding data window length and sampling frequency further reinforced the robustness and adaptability of the technique. The results show that the technique can accurately identify the faulty phase without being affected by operational disturbances.

Data availability

The datasets generated during and/or analyzed during the current study are available from the corresponding author on reasonable request.

Received: 20 March 2025; Accepted: 14 July 2025

Published online: 18 July 2025

References

1. Tiseo, I. Distribution of carbon dioxide emissions produced by the transportation sector worldwide in 2023, by sub sector. <https://www.statista.com/statistics/1185535/transport-carbon-dioxide-emissions-breakdown> (2025).
2. International Energy Agency. Aviation. <https://www.iea.org/energy-system/transport/aviation>, 2025.
3. Parhamfar, M., Sadeghkhani, I. & Adeli, A. M. Towards the net zero carbon future: A review of blockchain-enabled peer-to-peer carbon trading. *Energy Sci. Eng.* **12**(3), 1242–1264 (2024).
4. Setlak, L., Kowalik, R., Gebura, A. & Golda, P. Dynamic stability analysis of the aircraft electrical power system in the more electric aircraft concept. *Sci. Rep.* **14**(1), 25521 (2024).
5. Jones, C. E. et al. Electrical and thermal effects of fault currents in aircraft electrical power systems with composite aerostructures. *IEEE Trans. Transp. Electr.* **4**(3), 660–670 (2018).
6. Zhou, Q., Sumner, M. & Thomas, D. Fault location for aircraft distribution systems using harmonic impedance estimation. *IET Electr. Syst. Transp.* **2**, 119–129 (2012).
7. Andrea, J., Buffo, M., Guillard, E., Landfried, R., Boukadoum, R. & Teste, P. Arcing fault in aircraft distribution network. in *IEEE Holm Conference on Electrical Contacts* 317–324 (2017).
8. Mordor Intelligence. More electric aircraft market size & share analysis - Growth trends & forecasts (2025 - 2030). <https://www.mordorintelligence.com/industry-reports/more-electric-aircraft-market> (2025).
9. Smith, P., Furse, C. & Gunther, J. Analysis of spread spectrum time domain reflectometry for wire fault location. *IEEE Sens. J.* **5**(6), 1469–1478 (2005).
10. Yaramasu, A., Cao, Y., Liu, G. & Wu, B. Aircraft electric system intermittent arc fault detection and location. *IEEE Trans. Aerosp. Electron. Syst.* **51**(1), 40–51 (2015).
11. Li, T., Jiao, Z., Wang, L. & Mu, Y. A method of DC arc detection in all-electric aircraft. *Energies* **13**(16), 4190 (2020).
12. Thomas, J., Telford, R., Norman, P. J. & Burt, G. M. Intermittent series direct current arc fault detection in direct current more-electric engine power systems based on wavelet energy spectra and artificial neural network. *IET Electr. Syst. Transp.* **12**(3), 197–208 (2022).
13. Jiang, J., Zhao, M., Wen, Z., Zhang, C. & Albarracín, R. Detection of DC series arc in more electric aircraft power system based on optical spectrometry. *High Voltage* **5**(1), 24–29 (2020).
14. Rufato, R. C., Ditchi, T., de Steen, C. V., Lebey, T. & Oussar, Y. DC serial arc fault recognition in aircraft using machine learning techniques. *Int. J. Electr. Power Energy Syst.* **164**, 110408 (2025).
15. Seeley, D., Sumner, M., Thomas, D. W. & Greedy, S. DC series arc fault detection using fractal theory. in *IEEE International Conference on Electrical Systems for Aircraft, Railway, Ship Propulsion and Road Vehicles & International Transportation Electrification Conference (ESARS-ITEC)* (2023).
16. Kusic, G. Aircraft electrical monitoring & fault detection. in *ICINCO* (2) 133–141 (2004).
17. Li, W., He, K., Liu, W., Zhang, X. & Dong, Y. A fast arc fault detection method for AC solid state power controllers in MEA. *Chin. J. Aeronaut.* **31**(5), 1119–1129 (2018).
18. Chabert, A., Bakkay, M., Schweitzer, P., Weber, S. & Andrea, J. A transformer neural network for AC series arc-fault detection. *Eng. Appl. Artif. Intell.* **125**, 106651 (2023).
19. Laib, A. et al. Enhanced artificial intelligence technique for soft fault localization and identification in complex aircraft microgrids. *Eng. Appl. Artif. Intell.* **127**, 107289 (2024).
20. Tiwari, S. P. An adaptive and reliable protection scheme for critical fault detection in IEC microgrid considering dissimilar AC faults and weather-based random scenarios. *Electr. Eng.* **106**(5), 6373–6387 (2024).
21. Tiwari, S. P. An efficient protection scheme for critical fault detection in microgrid under uncertain scenarios using deep learning algorithm. *Electr. Eng.* 1–15 (2024).
22. Dai, W., Zhou, X., Sun, Z. & Zhai, G. Series alternating current arc fault detection method based on relative position matrix and deep convolutional neural network. *Eng. Appl. Artif. Intell.* **136**, 108874 (2024).
23. Radmanesh, H. & Kavousi, A. Aircraft electrical power distribution system protection using smart circuit breaker. *IEEE Aerosp. Electron. Syst. Mag.* **32**(1), 30–40 (2017).
24. TechSci Research. Aircraft electrical solid state power controller SSPC market size, share and forecast. <https://www.techsciresearch.com/report/aircraft-electrical-solid-state-power-controller-sspc-market/22790.html> (2025).
25. Moher, M. & Gulliver, T. Cross-entropy and iterative decoding. *IEEE Trans. Inf. Theory* **44**(7), 3097–3104 (1998).
26. Zamani, M. A., Yazdani, A. & Sidhu, T. S. A communication-assisted protection strategy for inverter-based medium-voltage microgrids. *IEEE Trans. Smart Grid* **3**(4), 2088–2099 (2012).
27. Benmouy, G. & Roberts, J. Superimposed quantities: Their true nature and application in relays. in *26th Annual Western Protective Relay Conference* (Spokane, 1999).
28. Abdel-Fadil, R., Eid, A., & Abdel-Salam, M. Electrical distribution power systems of modern civil aircrafts. in *2nd International Conference on Energy Systems and Technologies* 201–210 (2013).
29. Pagonis, M. Electrical power aspects of distributed propulsion systems in turbo-electric powered aircraft. Ph.D. dissertation, Cranfield University (2015).

Author contributions

S.H.: Writing – original draft, Software, Investigation, Formal analysis. I.S.: Writing – review & editing, Visualization, Supervision, Software, Methodology, Conceptualization. All authors reviewed the manuscript.

Competing interests

The authors declare no competing interests.

Additional information

Correspondence and requests for materials should be addressed to I.S.

Reprints and permissions information is available at www.nature.com/reprints.

Publisher's note Springer Nature remains neutral with regard to jurisdictional claims in published maps and institutional affiliations.

Open Access This article is licensed under a Creative Commons Attribution-NonCommercial-NoDerivatives 4.0 International License, which permits any non-commercial use, sharing, distribution and reproduction in any medium or format, as long as you give appropriate credit to the original author(s) and the source, provide a link to the Creative Commons licence, and indicate if you modified the licensed material. You do not have permission under this licence to share adapted material derived from this article or parts of it. The images or other third party material in this article are included in the article's Creative Commons licence, unless indicated otherwise in a credit line to the material. If material is not included in the article's Creative Commons licence and your intended use is not permitted by statutory regulation or exceeds the permitted use, you will need to obtain permission directly from the copyright holder. To view a copy of this licence, visit <http://creativecommons.org/licenses/by-nc-nd/4.0/>.

© The Author(s) 2025